

^{13}C NMR studies of the normal and superconducting states of the organic superconductor $\kappa\text{-(ET)}_2\text{Cu}[\text{N}(\text{CN})_2]\text{Br}$

S. M. De Soto and C. P. Slichter

Department of Physics and Materials Research Laboratory, University of Illinois at Urbana-Champaign, 1110 West Green Street, Urbana, Illinois 61801-3080

A. M. Kini, H. H. Wang, U. Geiser, and J. M. Williams

Chemistry and Materials Science Division, Argonne National Laboratory, Argonne, Illinois 60439

(Received 6 July 1995)

The authors report ^{13}C NMR spin-lattice relaxation rates $1/T_1$ and Knight shifts K_S in the quasi-two-dimensional organic superconductor $\kappa\text{-(ET)}_2\text{Cu}[\text{N}(\text{CN})_2]\text{Br}$ ($T_c = 11.6$ K), for an aligned single crystal. The normal-state behavior is reminiscent of the high- T_c cuprates, in which antiferromagnetic fluctuations and spin-gap behavior dominate. In the superconducting state, the data rule out the BCS electron-phonon mechanism as the source of the superconductivity, but support an unconventional pairing state with possible nodes in the gap function.

The discovery of superconductivity in organic charge-transfer salts based on the BEDT-TTF (“ET”) molecule has stimulated interest in understanding the electronic structure of their normal and superconducting states.¹ The ET compound with the highest ambient pressure critical temperature is $\kappa\text{-(ET)}_2\text{Cu}[\text{N}(\text{CN})_2]\text{Br}$ ($T_c = 11.6$ K).² This salt has a layered structure and quasi-two-dimensional (2D) electronic conduction, similar to the cuprate superconductors. The reduced dimensionality, and low carrier density ($\sim 10^{21}$ cm⁻³), indicate that electron correlation effects may be important. The nature of the superconducting state in the ET salts (i.e., BCS or unconventional) is unsettled at present. The low-temperature magnetic penetration depth has been studied, with some experiments supporting the existence of an isotropic BCS gap,³ and others an anisotropic gap.⁴

We have utilized ^{13}C NMR to study the normal and superconducting states of $\kappa\text{-(ET)}_2\text{Cu}[\text{N}(\text{CN})_2]\text{Br}$ [“ $\kappa\text{-(ET)}_2\text{Br}$ ”]. In agreement with the work of Mayafre *et al.*⁵ and Kawamoto *et al.*,⁶ we find that the normal-state behavior is not that of a simple metal, and that antiferromagnetic fluctuations, and spin-gap behavior may be present. Our data for $\kappa\text{-(ET)}_2\text{Br}$ below T_c favor spin-singlet pairing, and a highly anisotropic energy gap, such as is present for d -wave, or anisotropic s -wave, orbital pairing. Thus, in contrast to the $A_3\text{C}_{60}$ ($A = \text{K, Rb, Cs}$) “Buckyball” superconductors, the superconductivity in $\kappa\text{-(ET)}_2\text{Br}$ arises from a mechanism other than the conventional BCS electron-phonon coupling.

In a metal, the hyperfine interactions of the nuclei with the spins of the conduction electrons dominate the NMR properties. We find that in $\kappa\text{-(ET)}_2\text{Br}$, both the isotropic Fermi contact and anisotropic dipolar ($2p_z$) interactions are present. For a simple metal, the Korringa law relates the Knight shift K_S to the spin-lattice relaxation time $T_1: 1/T_1 T \propto K_S^2$. Below T_c , a gap opens at the Fermi level, producing dramatic changes in the NMR properties.⁷ For BCS spin-singlet s -wave superconductors, K_S decays

to zero as $T \rightarrow 0$ in a characteristic way.⁸ Just below T_c , $1/T_1$ rises (“coherence peak”), but falls off exponentially at low T .⁹ These features are found in the NMR studies of $A_3\text{C}_{60}$, clearly identifying it as a conventional BCS superconductor with an isotropic energy gap.¹⁰ We note that the above results are drastically modified in the case of an anisotropic gap function.

Previously, we have reported ^1H NMR in the superconducting state of $\kappa\text{-(ET)}_2\text{Br}$.¹¹ We showed that the NMR relaxation rates at these sites are dominated by fluxoid effects. In contrast to the ^1H sites, which are far from the region of high conduction-electron density, the central carbon atoms under observation are ideal for probing the superconducting electron wave function.

In this paper, we report ^{13}C NMR studies in an aligned single crystal (~ 2 mg) of $\kappa\text{-(ET)}_2\text{Br}$ for temperatures $2 \leq T \leq 300$ K and static magnetic fields $0.6 \leq H_0 \leq 8.3$ T. The two central carbon sites of the ET molecule (which have the largest conduction-electron density¹²) have been labeled with ^{13}C ($I = 1/2$).¹³ The measurements have been performed at 8.3 T in an Oxford superconducting magnet, and at 0.6 T in a Varian electromagnet using a 40 spin-echo-train Carr-Purcell sequence to enhance the poor S/N ratio for a single crystal in low field.¹⁴ For T_1 measurements, the nuclear magnetization was measured at a variable time after saturation or inversion of the resonance.

The quasi-2D crystal structure of $\kappa\text{-(ET)}_2\text{Br}$ is orthorhombic with alternating conducting layers (a face-to-face network of ET molecules) and insulating layers (composed of $\{\text{Cu}[\text{N}(\text{CN})_2]\text{Br}\}_\infty$ polymeric chains) both lying in the a - c plane, and staggered along the weakly conducting b axis at 15 Å intervals.¹⁵ In $\kappa\text{-(ET)}_2\text{Br}$, the ET molecules are paired in dimers (Fig. 1), which causes the two central ^{13}C sites of an individual molecule to become nonequivalent, producing two ^{13}C resonance lines. We designate these sites “inner” and “outer,” where the inner site is closer to the center of the dimer. There is

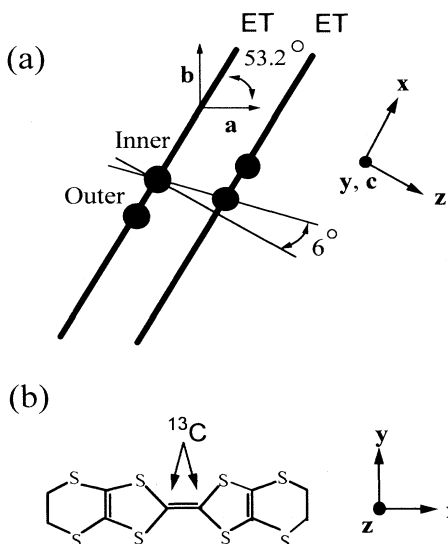


FIG. 1. (a) The dimer structure of $\kappa\text{-(ET)}_2\text{Cu}[\text{N}(\text{CN})_2]\text{Br}$. The heavy lines represent the x axis of the ET molecules and the circles locate the central ^{13}C sites under study. (b) The ET molecule, with ^{13}C sites indicated.

also a dipolar splitting of the resonance lines by the coupling to the nearest ^{13}C neighbor. Lastly, there are four magnetically inequivalent molecular orientations in the unit cell, so that 16 lines are observed for an arbitrary crystal orientation. For certain orientations, the dipole coupling is comparable to the magnetic shift difference between the inner and outer site, which causes the dipolar split lines to have significantly different intensities and T_1 times.

For $H_0 \parallel a$, the dipole splitting vanishes and the four orientations become equivalent, so that only two lines are observed. At room temperature, the lines are narrow (~ 12 ppm), and well separated (~ 130 ppm), broadened only by the ^{13}C dipolar coupling. A transition takes place near 150 K, below which the lines broaden dramatically.⁵ In Fig. 2, we show the temperature dependence of the ^{13}C linewidths (the inset shows the spectrum at 30 K with $H_0 \parallel a$). From an angular study of the line positions, we found that the principle axes of the shift tensors for the two sites differ slightly. The axes of the upper line coincide with those of the ET molecule, while the axes of the lower line are rotated out of the plane of the molecule by $\sim 6^\circ$. Based on the geometry of the dimer, we identify the lower (upper) line with the inner (outer) site. Relative to the inner line, the outer line is broader and has a larger shift.

We have measured the ^{13}C spin-lattice relaxation rate and shift tensors at $T=295$ K with $H_0=8.3$ T. The NMR total shift tensor in a metal is the sum of the chemical (orbital) and Knight- (spin) shift tensors. The chemical shift is proportional to the electron-spin-resonance g shift, which has been found to be independent of temperature in $\kappa\text{-(ET)}_2\text{Br}$ for $H_0 \parallel a$,¹⁶ so that $\vec{K}_{\text{TOT}}(T) = \vec{K}_{\text{CHEM}} + \vec{K}_S(T)$. The results are

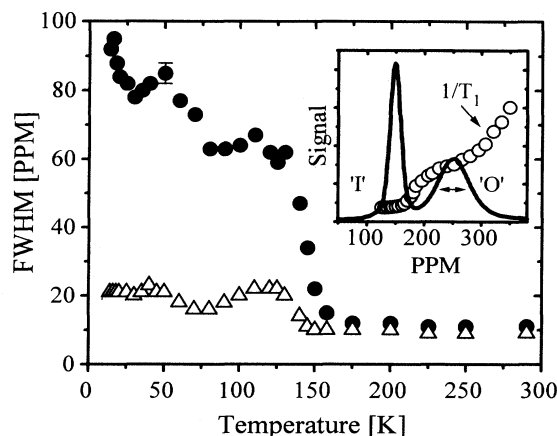


FIG. 2. The temperature dependence of the linewidth at the inner (triangles) and outer (circles) sites. Inset: ^{13}C NMR FFT line shape at $T=30$ K, with $H_0=8.3$ T and $H_0 \parallel a$. The relaxation rate $1/T_1$ vs shift is also shown (circles).

$\vec{K}_{\text{TOT}}^{\text{outer}} = (K_{\text{TOT}}^{xx}, K_{\text{TOT}}^{yy}, K_{\text{TOT}}^{zz}) = (121, 145, 754) \pm 20$ and $\vec{K}_{\text{TOT}}^{\text{inner}} = (9, 43, 449) \pm 20$ [all shifts are given in ppm, relative to tetramethylsilane (TMS)]. The shift tensor for pure ET (for which $\vec{K}_S=0$) is $\vec{K}_{\text{CHEM}}^{\text{ET}} = (66, 178, 26)$.¹² Assuming that the chemical shifts are nearly the same in $\kappa\text{-(ET)}_2\text{Br}$ (which is implied by our measurements near $T=0$), we obtain the following Knight-shift tensor $\vec{K}_S^{\text{outer}} = (55, -33, 728) \pm 25$ and $\vec{K}_S^{\text{inner}} = (-57, -135, 423) \pm 25$. The outer site relaxation rate ($W_1 \equiv 1/T_1$) tensor at 295 K has axial symmetry: $(W_1^x, W_1^y, W_1^z) = (53.8 \pm 2.5, 52.9 \pm 2.5, 1.35 \pm 0.10) \text{ sec}^{-1}$. The rates for the two in-plane axes are nearly equal and are much faster than that of the out-of-plane axis. This anisotropy arises from the combined isotropic Fermi contact field and the dipole field of the on-site $2p_z$ conduction-electron density, which reinforce in the z direction, but nearly cancel for x and y , i.e., $K_{s,zz} \gg K_{s,xx}, K_{s,yy}$. The relaxation rate is given by the sum of the perpendicular Knight shifts, e.g., $W_1^z \propto K_{s,xx}^2 + K_{s,yy}^2$, which explains why $W_1^z \ll W_1^x, W_1^y$.¹⁷ There are also small fields $\sim 5\%$ from the neighboring carbon and sulfur spin densities, which affect both K_s and $1/T_1$.

Below 150 K, the linewidth is much broader (in kHz) in high field than low field. Evidence that the high-field linewidth results from a distribution of spin shifts is shown in the inset of Fig. 2. Ordinarily, $1/T_1$ does not vary across a resonance line, but here ^{13}C nuclei with large (small) spin shifts have correspondingly fast (slow) relaxation rates. The distribution of resonance frequencies and relaxation rates is evidence for a spatial variation of either the charge or spin density of the conduction electrons. A similar broadening in $\beta\text{-(ET)}_2\text{I}_3$ below 200 K was proposed to result from a disordered electrostatic potential associated with the freezing of the motion of the terminal ethylene groups of the ET molecules (weak Anderson localization).¹⁸

In Fig. 2, the extra line broadening persists at low temperatures ($2 \text{ K} < T < 50 \text{ K}$) where the spin susceptibility

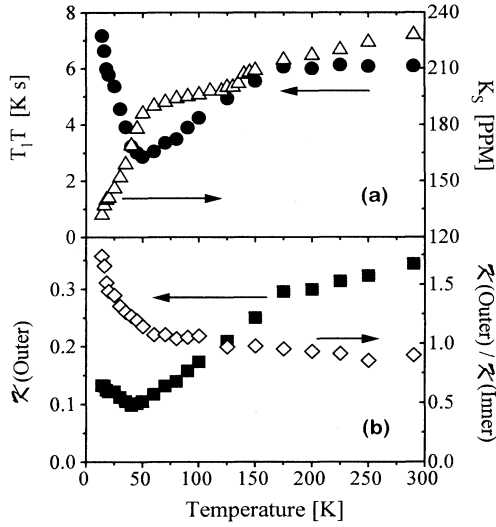


FIG. 3. (a) The temperature dependence of the Korringa product, T_1T (circles), and the Knight shift, K_s (triangles), for the outer site, with $H_0=8.3$ T and $H_0\parallel a$. We have assumed $K_{\text{CHEM}}^{\text{aa}}=96$ ppm. (b) The temperature dependence of the Korringa factor $\mathcal{K}^{\text{outer}}$ (squares) and the ratio $\mathcal{K}^{\text{outer}}/\mathcal{K}^{\text{inner}}$ (diamonds) for $H_0\parallel a$, $H_0=8.3$ T.

(Knight shift) is rapidly decreasing (Fig. 3), in conflict with the idea that the broad lines result from a distribution of electronic charge density (e.g., charge-density wave or weak localization). Another possibility is a spin-density wave (SDW). The nearly Gaussian line shape suggests a 2D SDW, since for a 1D SDW the line shape has sharp peaks at the upper and lower cutoff frequencies. Interestingly, the linewidth decreases below 50 K, reaching a minimum at 25 K, below which it increases once again. There are also “kinks” in both T_1T and K_s near these same temperatures (Fig. 3). Magnetic transitions have been reported in the isostructural compound $\kappa\text{-(ET)}_2\text{Cu[N(CN)}_2\text{]Cl}$ ($T_c=13$ K, “ $\kappa\text{-(ET)}_2\text{Cl}$ ”) at just these same temperatures: an antiferromagnetically (AF) ordered state below 45 K, and a transition to a weakly ferromagnetic state below $T=22$ K.¹⁹ Our data suggest that there are corresponding transitions in $\kappa\text{-(ET)}_2\text{Br}$, at least in high field (8 T). The SDW state may be induced by the magnetic field because the low-field (0.6 T) line shape is narrow (~ 1 kHz). Such phenomena have been found in the quasi-1D organic conductors based on the TMTSF molecule,²⁰ but not in the quasi-2D ET-based materials.

In Fig. 3, we show the temperature dependence of the ^{13}C T_1T and K_s , for the outer site, with $H_0=8.3$ T and $H_0\parallel a$, where the relaxation rate is measured at the peak of the resonance line (Fig. 2). Our results are similar to those previously reported.^{5,6} Above 150 K, $T_1T\sim\text{const}$ and K_s is slowly varying, typical for metallic systems. The kink in K_s at 135 K coincides with the line broadening transition, while the rapid decrease of K_s below 50 K reflects a freezing out of the spin susceptibility.¹⁶ The

linear- T dependence of T_1T from 45 to 150 K is similar to the high- T_c cuprates, which are dominated by antiferromagnetic fluctuations and the existence of a spin gap.²¹ The T_1T minimum near $T=50$ K corresponds to the temperature of the spin-susceptibility drop. The Korringa factor describing electron correlations is $\mathcal{K}=(T\|T|K_{\perp}|^2)_{\text{experimental}}/(\hbar\gamma_e^2/4\pi k_B\gamma_n^2)$. For a free-electron gas, $\mathcal{K}=1$. For the outer site, with $H_0\parallel x$, we find $\mathcal{K}^{\text{outer}}(300\text{ K})=0.34$. In Fig. 3(b), we show $\mathcal{K}^{\text{outer}}(T)$ and the ratio $\mathcal{K}^{\text{outer}}(T)/\mathcal{K}^{\text{inner}}(T)$ scaled by using the temperature dependence of $T_{1a}(T)$ and $K_s^{\text{aa}}(T)$. Values of $\mathcal{K}<1$ are evidence for an antiferromagnetic reduction of the spin susceptibility, which, from our data becomes more pronounced as T is lowered. The site ratio is roughly constant above 50 K, but then diverges strongly below this transition temperature, indicating the onset of different physics at the two sites. Lastly, we note that the Korringa relationship (using our Knight-shift values) implies a ratio for the outer to inner site $1/T_1$ of 2.65, close to the experimental room-temperature value of 3.0.

We turn now to the superconducting state. In Fig. 4, we show the temperature dependence of $\ln(1/T_1)$ vs $1/T$ with $H_0\parallel a$ for two values of the external field, $H_0=0.6$, 8.3 T. There are three striking aspects to the data. (1) There is a field dependence to $1/T_1$. In our previous ^1H NMR in $\kappa\text{-ET}_2\text{Br}$, as well as in the cuprates, it has been shown that fluxoids in the mixed state of a type-II superconductor can provide an additional contribution to the relaxation rate.^{11,22} It is assumed that the low-field data give a closer approximation to the zero-field limit to which theory applies. In Fig. 4, we show at 3 K a “zero-field” point calculated by extrapolation assuming a linear field dependence.²² The point lies close to the low-field rate. (2) There is no coherence peak just below T_c . Instead, $1/T_1$ drops sharply upon entering the superconducting state. It has been shown that electron-spin scattering may reduce the coherence peak, with the effect

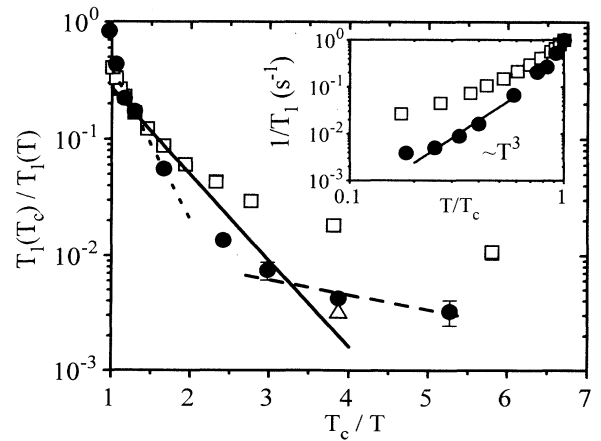


FIG. 4. The temperature dependence of the spin-lattice relaxation rate in the superconducting state, with $H_0\parallel a$, and $H_0=8.3$ T (squares) and $H_0=0.6$ T (circles). A “zero-field” extrapolation point (triangle) is shown. Inset: The data on a log-log plot.

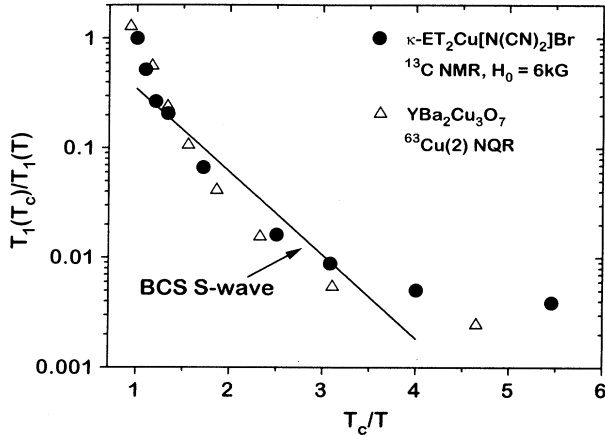


FIG. 5. A comparison of the superconducting state behavior of the spin-lattice relaxation rate in $\kappa\text{-(ET)}_2\text{Cu[N(CN)}_2\text{]Br}$, and $\text{YBa}_2\text{Cu}_3\text{O}_7$ (a typical cuprate superconductor). The rates have been scaled to their values at T_c . Neither set of data follows the exponential BCS slope at low temperatures.

being more pronounced for pairing states with nodes in the energy gap.²³ (3) The data do not lie on a straight line at lower temperatures, as required for an isotropic s -wave superconductor: $1/T_1 \propto \exp(-\Delta/k_B T)$. The weak-coupling BCS slope $\Delta(0)/k_B T_c = 1.76$ is indicated in Fig. 4. Just below T_c the experimental slope in low field is 3.0, while at low T the slope is reduced to 0.3. The changing slope may be accounted for by anisotropies of the gap in \mathbf{k} space. We can estimate the ratio of the maximum and minimum gap sizes, from the slope ratios,²⁴ to be at least $3.0/0.3 = 10$.

The temperature dependence of $1/T_1$ therefore rules out the possibility of an isotropic BCS s -wave energy gap. For an orbital d -wave pairing state, we expect that $1/T_1 \propto T^3$ at low T . In the inset of Fig. 4, we plot $\ln(1/T_1)$ vs $\ln T$. The low-field data reasonably fit the T^3 law for much of the temperature range. The lowest data point lies just above the line, indicating that there may be another contribution (e.g., fluxoids, impurities) at the lowest temperatures. We note that quite similar behavior is seen in $\text{YBa}_2\text{Cu}_3\text{O}_7$, which very likely has a $d_{x^2-y^2}$ pairing state. In fact, in Fig. 5, we compare our relaxation rate data for $\kappa\text{-(ET)}_2\text{Cu[N(CN)}_2\text{]Br}$ directly with ^{63}Cu NQR data of Corey in our laboratory for $\text{YBa}_2\text{Cu}_3\text{O}_7$. The similarity is indeed striking, indicating the lack of conventional BCS behavior in both systems.

We turn now to the Knight shift below T_c . For a spin-singlet superconductor, $\chi_s \rightarrow 0$ as $T \rightarrow 0$, so that $\vec{K}_{\text{TOT}}(T=0) = \vec{K}_{\text{CHEM}}$. A complication is that the internal magnetic field in a type-II superconductor is slightly less than the applied field ($B_{\text{int}} \neq H_0$), because of the diamagnetic screening currents. The maximum difference is given by the lower critical field, $H_{c1} \approx 1 \text{ G}$.³ Furthermore, for the field applied parallel to the superconducting layers, the demagnetization correction should be small. For these reasons, we will make the approximation that $B_{\text{int}} = H_0$ and ignore any diamagnetic corrections for the

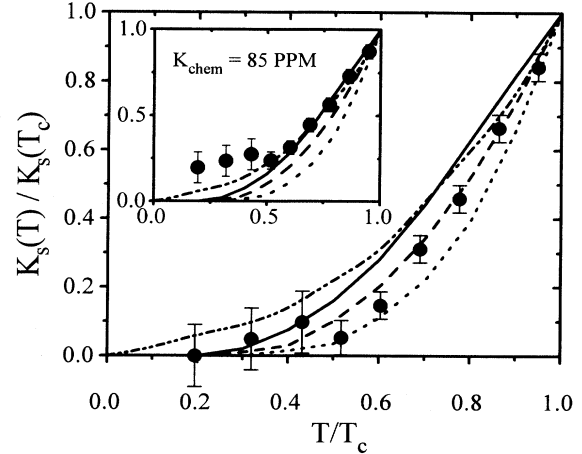


FIG. 6. The Knight shift in the superconducting state for the inner site, with $H_0 = 8.3 \text{ T}$, and $H_0 \parallel a$, using $K_{\text{CHEM}}^{aa} = 96 \text{ ppm}$. The fits shown are BCS s -wave weak-coupling (solid), strong-coupling s -wave with $T_c/\omega_{\text{ph}} = 0.1$ (dashed), $T_c/\omega_{\text{ph}} = 0.3$ (dotted), and strong-coupling, spin-singlet, d -wave pairing (dot-dash) (Ref. 22). Inset: Rescaled Knight-shift data using $K_{\text{CHEM}}^{aa} = 85 \text{ ppm}$.

^{13}C resonance frequency below T_c . The shift tensors measured for $T \sim 3 \text{ K}$ (i.e., $T \rightarrow 0$) are $\vec{K}_{\text{TOT}}^{\text{inner}} = (K_{aa}^{\text{inner}}, K_{bb}^{\text{inner}}, K_{cc}^{\text{inner}}) = (96 \pm 3, 35 \pm 6, 105 \pm 5)$ and $\vec{K}_{\text{TOT}}^{\text{outer}} = (100 \pm 3, 154 \pm 6, 105 \pm 5)$. For comparison, the chemical shift tensor for pure ET is $\vec{K}_{\text{CHEM}}^{\text{aa}} = (85, 83, 102)$. For $H_0 \parallel a, c$ the collapse of both lines close to the shift of pure ET argues that $\chi_s^{aa}(0) = 0$ and $\chi_s^{cc}(0) = 0$. Since for $H_0 \parallel a, c$ all three principal components x, y, z of the ET molecules are sampled, this is evidence that the tensor $\vec{\chi}(0) = 0$. Evidently, for $H_0 \parallel b$, the applied field produces a physical change in the electron system, such that a residual magnetic field remains, which is different at the two sites. These data cannot be explained by the so-called planar state, which displays anisotropic susceptibility.²⁵

In Fig. 6, we show the normalized temperature dependence of the inner site ^{13}C Knight shift below T_c for $H_0 \parallel a$, assuming $K_{\text{chem},aa}^{\text{inner}} = 96 \text{ ppm}$, with fits for s - and d -wave pairing states and various coupling strengths (T_c/ω_{ph}), where ω_{ph} is a typical phonon frequency.²⁶ The large uncertainties at low T result from the gradual overlap of the inner and outer resonance lines. The inset shows the same data assuming $K_{\text{chem},aa}^{\text{inner}} = 85 \text{ ppm}$, the pure ET value. The inset situation might arise from impurities, as has been shown by Ishida for Zn-doped $\text{YBa}_2\text{Cu}_3\text{O}_7$.²⁷ Experience with the cuprates has shown that it is difficult to determine the orbital pairing state from $K_s(T)$. In contrast, the spin-lattice-relaxation rate results below T_c cannot be reconciled with a conventional BCS isotropic s -wave superconducting pairing state.

The authors thank T. Imai, R. Corey, N. Curro, C. Milling, V. Barzykin, A. Sokol, and D. Pines for many

helpful discussions. This work has been supported through the University of Illinois Materials Research Laboratory by a grant from the DOE Division of Materials Research under Grant No. DEFG02-91ER45439 (S.M.D., C.P.S.) and the Science and Technology Center

for Superconductivity under Grant No. DMR 91-20000 (C.P.S.) and through Argonne National Laboratory by the DOE Division of Material Science under Contract No. W-31-109-ENG-38 (A.M.K., H.H.W., U.G., J.M.W.).

-
- ¹T. Ishiguro and K. Yamaji, *Organic Superconductors* (Springer-Verlag, New York, 1990).
- ²A. M. Kini *et al.*, *Inorg. Chem.* **29**, 2555 (1990).
- ³M. Lang *et al.*, *Phys. Rev. B* **46**, 5822 (1992).
- ⁴T. Takahashi, K. Kanoda, and G. Saito, *Physica C* **185-189**, 366 (1991).
- ⁵H. Mayafre *et al.*, *Europhys. Lett.* **28**, 205 (1994).
- ⁶A. Kawamoto *et al.*, *Phys. Rev. Lett.* **74**, 3455 (1995).
- ⁷J. Bardeen, L. N. Cooper, and J. R. Schrieffer, *Phys. Rev.* **108**, 1175 (1957).
- ⁸K. Yosida, *Phys. Rev.* **110**, 769 (1958).
- ⁹L. C. Hebel and C. P. Slichter, *Phys. Rev.* **113**, 1504 (1959).
- ¹⁰A. V. Stenger *et al.*, *Phys. Rev. Lett.* **74**, 1649 (1995).
- ¹¹S. M. De Soto *et al.*, *Phys. Rev. Lett.* **70**, 2956 (1993).
- ¹²T. Klutz *et al.*, *Appl. Magn. Reson.* **2**, 441 (1991).
- ¹³K. D. Carlson *et al.*, *Inorg. Chem.* **31**, 3346 (1992).
- ¹⁴S. E. Barrett *et al.*, *Phys. Rev. B* **41**, 6283 (1990).
- ¹⁵U. Geiser *et al.*, *Acta Crystallogr. C* **47**, 190 (1991).
- ¹⁶V. Kataev *et al.*, *Solid State Commun.* **83**, 435 (1992).
- ¹⁷See, e.g., C. P. Slichter, *Principles of Magnetic Resonance*, 3rd ed. (Springer-Verlag, New York, 1990), p. 197.
- ¹⁸A. V. Vainrub *et al.*, *Phys. Rev. Lett.* **69**, 3116 (1992).
- ¹⁹U. Welp *et al.*, *Phys. Rev. Lett.* **69**, 840 (1992).
- ²⁰D. Jerome, *Science* **252**, 1509 (1991).
- ²¹A. J. Millis, H. Monien, and D. Pines, *Phys. Rev. B* **42**, 167 (1990); A. Sokol and D. Pines, *Phys. Rev. Lett.* **71**, 2813 (1993).
- ²²J. A. Martindale *et al.*, *Phys. Rev. Lett.* **68**, 702 (1992).
- ²³H. Monien and D. Pines, *Phys. Rev. B* **41**, 6297 (1990).
- ²⁴J. A. Martindale *et al.*, *J. Phys. Chem. Solids* **54**, 1439 (1993).
- ²⁵A. J. Leggett, *Rev. Mod. Phys.* **47**, 331 (1975).
- ²⁶R. Akis, C. Jiang, and J. P. Carbotte, *Physica C* **47**, 485 (1991); S. Barrett, Ph.D. thesis, University of Illinois, 1992.
- ²⁷K. Ishida *et al.*, *J. Phys. Soc. Jpn.* **62**, 2803 (1993).